ELSEVIER

Cement & Concrete Composites 24 (2002) 509–521

Cement & Concrete Composites

www.elsevier.com/locate/cemconcomp

Ultimate punching shear strength analysis of slab–column connections

D.D. Theodorakopoulos [a], R.N. Swamy [b,*]

[a] University of Patras, Patras, Greece

[b] Department of Mechanical Engineering, University of Sheffield, Mappin Street, P.O. Box 600, Sheffield S1 4DU, UK

Abstract

A simple analytical model is presented to predict the ultimate punching shear strength of slab–column connections. The model is based on the physical behavior of the connections under load, and is therefore applicable to both lightweight and normal weight concrete. The model assumes that punching is a form of combined shearing and splitting, occurring without concrete crushing, but under complex three dimensional stresses. Failure is then assumed to occur when the tensile splitting strength of the concrete is exceeded. The theory is applied to predict the ultimate punching shear strength of 60 slab–column connections reported recently in literature, and designed to fail in shear, involving a large number of variables, such as type of concrete, concrete strength, tension steel ratio, compression reinforcement and loaded area. The results show very good agreement between the predicted and experimental values. The uniqueness of the model is that it incorporates many physical characteristics of the slabs and their failure behavior, and this is reflected by its ability to predict extremely well the results of tests conducted by researchers other than the authors.

Keywords: Punching; Slab; High strength concrete; Compression zone; Aggregate interlock; Dowel action; Shear cracking; Neutral axis depth; Tensile splitting strength

1. Introduction

The problem of the punching shear strength of reinforced concrete slabs subjected to concentrated loads has received great attention over several decades because of its importance in flat plate floor systems. The ultimate strength of such slabs is often determined by the punching shear failure load, which is generally smaller than the flexural failure load calculated by theories such as the yield line theory. Many variables have a marked effect on the punching shear strength of slabs. These include the concrete strength, the ratio of the column size to slab effective depth, the ratio of shear strength to flexural strength, the column shape and the lateral constraints. Most research on the punching shear strength of slabs has been concerned with the generation of experimental data on simply supported slabs and the development of empirical equations. A few theoretical analyses have also been proposed by various investigators based on different models [1]. More recently, various authors have proposed different approaches to solve the punching shear problem, such as truss analogy [2], fracture analysis [3], finite element analysis [4] and the modified mechanical model of Kinnunen and Nylander [5]. The lack of a simple theoretical model is due to complexities of the basic three-dimensional behavior of the slab–column connection, and the uncertain shear transfer mechanism that exists in the slab before failure.

The purpose of this paper is to present a simple analytical model for the punching shear strength of slab–column connections. The concepts are developed in such a way that the model can be applied to both normal weight and lightweight concrete connections. The model incorporates a good representation of the physical behavior, under load, of slab–column connections. Punching is considered as a form of combined shearing and splitting, occurring without crushing, but under complex three dimensional stresses. Failure is then assumed to occur in the so-called compression zone above the inclined crack when the limiting shear stress equals

* Corresponding author. Tel.: +44-114-222-7712; fax: +44-114-222-7890.

E-mail address: r.n.swary@sheffield.ac.uk (R.N. Swamy).

0958-9465/02/$ - see front matter
PII: S0958-9465(01)00067-1

Nomenclature

b	unit width of slab section
b_n	beam width
b_p	control perimeter
d	effective depth
f_c	concrete cylinder strength
f_{ct}	tensile strength of concrete
f_{cu}	concrete cube strength
f_s	tension steel stress
f'_s	compression steel stress
f_y	steel yield stress
h	slab depth
k_1	concrete stress block parameter
l_c	critical length of the dowel action in a beam
r	column side
A	coefficient
B_n	net circular length at the level of reinforcement
D	column diameter
E	modulus of elasticity of steel
F_c	concrete stress block force
F_s	tension steel force
F'_s	compression steel force
X	neutral axis depth
X_f	depth of the compression zone of the flexural critical section
X_{fx}	depth of the compression zone of the flexural critical section in x direction
X_{fy}	depth of the compression zone of the flexural critical section in y direction
X_s	depth of the compression zone of the shear critical section
V_a	aggregate interlock force
V_c	vertical component of the compression zone resistance
V_{cc}	resistance of the compression zone
V_d	dowel action of flexural reinforcement
V_u	ultimate shear resistance of a slab
ε_{cu}	ultimate concrete strain
ε_o	concrete strain
ε_y	steel yield strain
θ	angle of failure surface
ρ	tension steel reinforcement ratio
ρ'	compression steel reinforcement ratio
φ	angle between flexural and shear sections
Φ	steel bar diameter

the tensile splitting strength of the concrete. The analysis involves the calculation of the depth of the compression zone, both in flexural and shear sections. Dowel action is taken into account by using a critical parameter at the level of the tension steel. It is shown that the analysis presented here advances a good theoretical model to predict the punching shear strength of reinforced concrete slabs.

2. Slab–column failure mechanism

Application of an increasing load to a slab which is monolithically connected to a column (i.e., slab to column or column to slab) within a slab–column–slab system implies the sequence of a number of events such as (1) the formation of a roughly circular crack around the column periphery on the tension surface of the slab and its subsequent propagation into the compression zone of the concrete, (2) formation of new lateral and diagonal flexural cracks, and (3) the initiation of an inclined shear crack near middepth of the slab, observed at about 50–70% of the ultimate load. With increasing loads the inclined crack develops towards the compression zone and the tension steel, but at the final stage, its propagation is prevented by the compression zone above the top of the crack near the column face and by the dowel action of the tension reinforcement. At this stage, slab tension steel close to the column yields, especially when realistic reinforcement percentages are used. Finally, punching shear failure occurs in the compression zone before yielding extends beyond the vicinity of the column. In the majority of test slabs reported in the literature, this failure in the compression zone occurred by splitting along the line AA′ and/or BB′ shown in Fig. 1(a), and there was no sign of concrete crushing. Punching is thus a form of shearing without shear–compression failure occurring.

Once inclined shear cracking has developed, the applied load is resisted by the vertical components of compression zone above the crack, V_c, the aggregate interlock force, V_a, and the dowel action of flexural reinforcement, V_d, Fig 1(a). Thus, the total shear resistance of a slab connection without shear reinforcement is given by

$$V_u = V_c + V_a + V_d. \quad (1)$$

In real slab–column connections these components do not remain isolated quantities, but co-exist together and, therefore, their contributions do not reach their maximum values at the same stage of loading, as experimental evidence in beams indicates [6].

The portion of the load resisted by the compression zone is dependent upon the area of slab above the in-

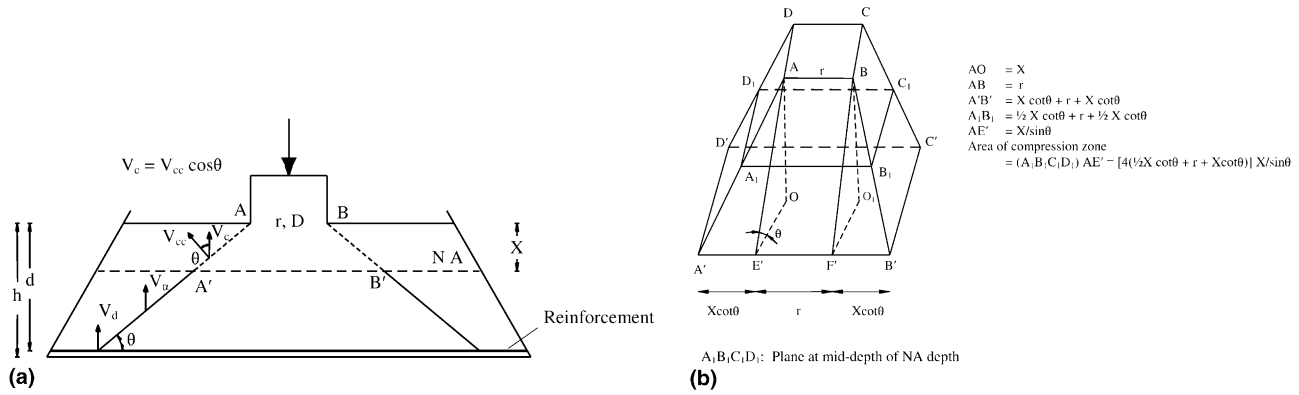

Fig. 1. Engineering model for punching shear.

clined crack, and the shear resistance of concrete. The aggregate interlock effect, which activates only after the appearance of inclined cracking, depends on concrete properties, crack width and the relative displacement between the two faces of crack due to rotation about the head of crack [6]. In slab–column connections, the movement across the crack at failure stages is largely vertical. However, the aggregate interlock force is activated only after the formation of the inclined crack, and the model neglects this *at failure* because of the "large" separation between the crack faces as observed in many tests and in practice. The dowel action contribution depends mainly on the tensile strength of concrete along the splitting plane at the reinforcement layer and the bending resistance of the steel [6–8].

3. Proposed ultimate strength analysis

Neglecting aggregate interlock contribution, Eq. (1) can be written as

$$V_u = V_c + V_d. \tag{2}$$

3.1. Resistance of compression zone

The resistance offered by the concrete compression zone, V_{cc}, is equal to that acting on an inclined, uncracked area of the concrete confined between the plane of the slab–column junction and the neutral axis (NA) plane. Considering the failure surface shown in Fig. 1(b), one obtains for a square column

$$V_{cc} = \left[4\left(\frac{1}{2}X\cot\theta + r + \frac{1}{2}X\cot\theta\right)\right]\frac{X}{\sin\theta}f_{ct}, \tag{3.1}$$

where r is the column side, X is the NA depth, θ is the angle of the failure surface, and f_{ct} is the tensile strength of concrete.

Tests show that the inclined cracking shape at the tension zone is in general an irregular one, and can be idealized in any form as various Code provisions do. In the model presumed here, an unified perimeter for both square and circular columns is adopted, primarily for the sake of generality but without any loss of accuracy. Indeed, the same predicted ultimate strength for two identical slabs except the column shape (square column, column area r^2 and a circular column with diameter $D = r$, column area $\pi D^2/4 < r^2$) highlights the concentration of stresses at column corners, leading to a reduction in shear capacity of the slabs with square column stub. Thus, for a circular column

$$V_{cc} = \left[4\left(\frac{1}{2}X\cot\theta + D + \frac{1}{2}X\cot\theta\right)\right]\frac{X}{\sin\theta}f_{ct}. \tag{3.2}$$

The NA depth depends on concrete strength properties and the amount and strength properties of the reinforcement. In the above expression the perimeter within the brackets is located at midway of the NA depth, X. Thus, the vertical component of the compression zone contribution to shear resistance, Fig. 1(a), is given by

$$V_c = \left[4\left(\frac{1}{2}X\cot\theta + r + \frac{1}{2}X\cot\theta\right)\right]X\cot\theta f_{ct} \tag{4.1}$$

or

$$V_c = \left[4\left(\frac{1}{2}X\cot\theta + D + \frac{1}{2}X\cot\theta\right)\right]X\cot\theta f_{ct}. \tag{4.2}$$

3.2. Contribution of the dowel action

The resistance offered by dowel action in two-way slabs has been reported to be about 25–35% of the ultimate resistance, based primarily on experimental evidence, since a purely theoretical evaluation of its magnitude is difficult with any degree of accuracy [7,8]. Bauman and Rüsch [7] derived a semi-empirical expression based on results of test beams specially designed to measure the dowel force of the flexural reinforcement. Their expression was modified later by Humadi and Regan [8] to include results of additional

tests. The experimentally defined dowel force was given by

$$V_d = b_n l_c f_{ct}, \tag{5.1}$$

where b_n is the width of the beam at the level of the reinforcement, and l_c is a critical length which depends on cube concrete strength properties, f_{cu}, and the diameter of steel bars, Φ, given by

$$l_c = \frac{4.12}{0.26}\Phi^{2/3}\frac{1}{f_{cu}^{1/3}}. \tag{5.2}$$

With regard to slab–column connections, Hallgren [5] in his proposed punching model used a similar equation for the calculation of the dowel force given by the general expression

$$V_d = B_n l_c f_{ct}, \tag{5.3}$$

where B_n is the corresponding net circular length at the level of reinforcement. It should be mentioned here that if the steel bars intersecting the shear crack yield, then the dowel force reduces considerably and, therefore, it remains an unknown quantity for any theoretical analysis.

Based on the above considerations and since both concrete compression zone and dowel action contributions depend on the same parameters, as the structure and nature of their Eqs. (4.1), (4.2) and (5.1)–(5.3) indicate, it is justifiable for the sake of simplicity and practicability, to consider these actions as a whole. It is thus logical to combine these two effects, particularly because the estimation of the dowel action effect is difficult, especially in the case of a slab where yielding of the tension reinforcement occurs. In the model presented here the dowel action effect is accounted for by incorporating a larger fictitious perimeter for use in Eqs. (4.1) and (4.2), and for convenience, the control parameter used in BS 8110 [9], is adopted here, i.e.,

$$b_p = [4(1.5d + r + 1.5d)] = 4r + 12d \tag{6.1}$$

or

$$b_p = [4(1.5d + D + 1.5d)] = 4D + 12d \tag{6.2}$$

in which d is the effective depth of the slabs. It should be mentioned that the use of a large perimeter away from the column face proposed by the British Codes (initially $1.5h$ and later $1.5d$), was adopted just to account for the dowel action of the flexural reinforcement [10]. In the light of this assumption, substitution of Eqs. (6.1) and (6.2) into Eqs. (4.1) and (4.2) respectively, yields

$$V_u = [b_p]X\cot\theta f_{ct} \tag{7}$$

which is the prediction equation for the ultimate punching strength.

4. Depth of the compression zone

The ability to determine the depth of the compression zone accurately at failure is the key to any satisfactory theory for ultimate strength. In slab connections, at the final stages of loading, both inclined and flexural cracking are prevented from propagating into the compression zone above. The two cracks are at the critical sections of the slab, for shear and moment, respectively, which are both at or very close to the column face, as shown schematically in Fig. 2. Thus, there is a strong moment–shear interaction influencing both the NA depth and the failure mode of the slab. Experimental evidence from tests on slabs shows that their mode of failure is strongly influenced by the tension steel reinforcement ratio, ρ. Those slabs which showed yielding of reinforcement in the vicinity of the column before punching had the quantity $\{f_{cu}/\rho f_y\}$ (where f_{cu} and f_y are the cube concrete strength and the steel yield stress, respectively) varying from 5.0 to 9.0, with the majority of values between 6.0 and 8.0. In this analysis it is assumed that for such slabs, the depth of the compression zone of the shear critical section at punching, X_s, is equal to the depth of the compression zone at flexure, X_f, under the condition of local yielding of the reinforcement i.e.,

$$X = X_s = X_f, \tag{8}$$

and X_f can be calculated by following the classical procedure for flexure.

For all other slabs, $X_s \neq X_f$, and then the problem arises as to which value of X should be used to calculate the ultimate punching shear strength. An answer should be possible if the exact mechanism of the moment–shear interaction in slabs is known. In its absence, we need a prescription to evaluate a "mean" value of NA depth X, in terms of X_s and X_f, which will, in effect, represent the overall real situation of the uncracked area of concrete in the loaded region. An arithmetic mean will be too simplistic and would lead to incorrect implications when, for example, the tension reinforcement varies. A harmonic mean, on the other hand, is physically more

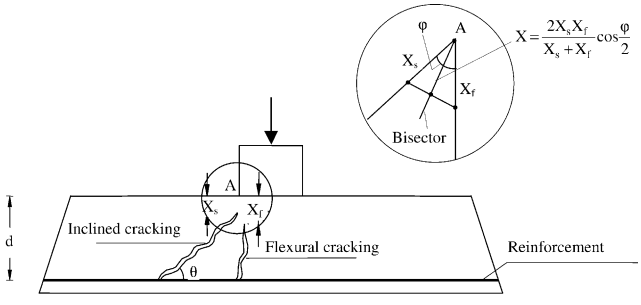

Fig. 2. Schematic presentation of cracking.

sensible, particularly in limiting cases. This harmonic mean is given by

$$\frac{1}{X}=\frac{1}{2X_s}+\frac{1}{2X_f} \tag{9}$$

or

$$X=\frac{2X_sX_f}{X_s+X_f}.$$

It is also easily proved, by trigonometry, that the "mean" value of NA depth X given by Eq. (9), is in essence, the depth of the concrete compression zone located at the bisector of the angle Φ, which is formed by shear and flexural cracking lines as shown in Fig. 2, when Φ tends to zero, i.e., when the two sections are very close to each other or coincide. The effectiveness of the use of the harmonic mean formulation can be quickly seen in the following two limiting cases.

1. Let $X_f \to 0$, that is, the amount of tension steel tends to zero. Then, Eq. (9) yields, $X \to 0$, and therefore Eq. (7) implies that the punching resistance of the slab is negligible, as expected. On the other hand, the arithmetic-mean formulation would have given a non-zero strength in this situation.
2. Let $X_f \gg X_s$, which is the case of heavily reinforced slabs. Then, Eq. (9) yields, $X \to 2X_s$, indicating that any further increase in the amount of steel above a limiting value offers negligible increase to punching resistance, as experimental evidence indicates [1,11]. Once again, it is easily seen that the arithmetic-mean formula would have retained the effect of X_f on X.

4.1. Depth of the shear critical section

Assuming an average value of the quantity $f_{cu}/\rho f_y$ equal to 7.0, it is easily shown that $X_f = 0.25d$, which implies (Eq. (8)) that the value of the shear critical section is equal to $0.25d$ as well, i.e.,

$$X_s = 0.25d. \tag{10}$$

It should be noted that, after considering the separate action of the two critical sections, it is only the depth X_f that is influenced by any variation in concrete properties and steel amount and properties, the depth X_s being unaffected. Thus, Eq. (10) is used for the calculation of the depth of the shear critical section, no matter what the properties of the concrete and steel are.

4.2. Depth of the flexural critical section

The computation of the NA depth of the flexural critical section, X_f, is based on the classical procedure for flexure used for normal density concrete except that the effect of steel strain hardening effect is recognized.

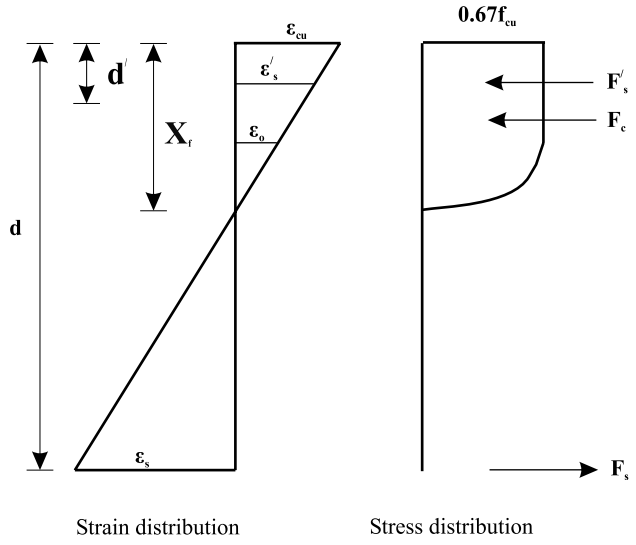

Fig. 3. Strain and stress distribution for concrete.

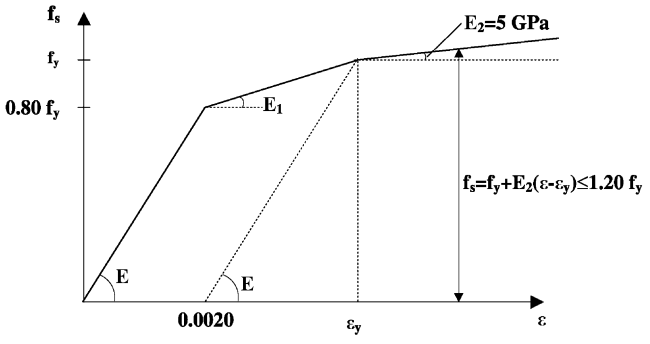

Fig. 4. Typical stress–strain curve for steel.

The assumed stress and strain distributions at failure for concrete are shown in Fig. 3, while Fig. 4 shows a typical stress–strain curve for steel. The resulting forces of the concrete stress block, F_c, as well as the forces of steel both in tension, F_s, and compression, F'_s , are as follows:

$$F_c = k_1 f_{cu} b X_f, \tag{11.1}$$

$$F_s = \rho f_s b d, \tag{11.2}$$

$$F'_s = \rho' f'_s b d, \tag{11.3}$$

and

$$F_s = F_c + F'_s, \tag{12}$$

where

$$X_f = \frac{\rho f_s - \rho' f'_s}{k_1 f_{cu}} d, \tag{13}$$

$$k_1 = 0.67\frac{\varepsilon_{cu} - A\varepsilon_o/3}{\varepsilon_{cu}}, \quad \varepsilon_o = \frac{\sqrt{f_{cu}}}{4115} \tag{14}$$

in which f_s and f'_s are the steel stresses in tension and compression respectively, ρ' is the reinforcement ratio of compression steel, ε_{cu} is the ultimate concrete strain, ε_o is

the concrete strain at the level of the end of the rectangular concrete stress block, b is the unit width of the slab, and the coefficient $A = 1$ for normal density concrete. The computation of f_s , f'_s and X_f follows an iterative procedure and uses the compatibility conditions and equilibrium equations given above.

5. Evaluation of f_{ct} and θ

In slab–column connections reference is often made to the strength of concrete in shear. However, concrete is a granular material, and the unqualified term "shear strength" applied to such a material is meaningless. It can be anything between the tensile strength and several times the compressive strength. Since punching is a form of combined shearing and splitting occurring in the compression zone under complex triaxial stresses, and since in simply supported slabs there is no membrane action present prior to the formation and completion of the full yield line mechanism, it is the unconstrained shear strength which is critical to punching failure. In this analysis, failure is assumed to occur when the shear stress exceeds the tensile splitting strength of concrete, f_{ct}, which can be expressed as a function of cube compressive strength, f_{cu}. Regan and Braestrup [1] in their analysis, showed that trends of the data of ultimate punching strength of slabs are reasonably well expressed by $V_u \propto f_{cu}^{1/3}$ or $V_u \propto f_{cu}^{1/2}$ while the expression $V_u \propto f_{cu}^{2/3}$ overestimates the influence of the compressive strength. However, this is true only if the isolated interrelation of f_{cu} and punching test results is examined. In reality, the concrete compressive strength does not only influence the limiting shear stress, but also the overall flexural behavior of the slab, although to a lesser degree, which in turn affects the punching resistance. The latter is taken into account, in the present analysis, through the calculation of X_f. Finally, f_{ct} is taken as [12]

$$f_{ct} = 0.27 f_{cu}^{2/3}. \tag{15}$$

The angle of the failure surface, θ, in slab–column connections of normal density concrete varies from 25° to 30°, although failures at steeper angles can occur without much apparent effect on the ultimate load. In test slabs made with high strength concrete, slopes of the failure shear crack of about 30–40° have been reported [5]. In the present analysis, a value of θ equal to 30° is assumed.

6. Mechanical properties for concrete and steel

To apply the proposed engineering model in order to predict the ultimate punching shear strength of slab–column connections, the knowledge of various mechanical properties for concrete and steel is required, which may not always be available. Thus, in what follows expressions are given for estimation of mean values of these properties.

6.1. Concrete

If the cylinder strength, f_c, is available as compressive strength of concrete, then the equivalent cube strength is estimated by

$$f_{cu} = f_c/0.80. \tag{16}$$

The conversion factor 0.80 in Eq. (16) seems to be an acceptable value on the safe side, even when high strength concrete is used [5].

The ultimate concrete strain in compression, ε_{cu}, is taken equal to 0.0035 for both lightweight and normal weight concrete. This value can also be used, for the sake of generality, in the case of high strength concrete, although lower values of ultimate strain have been experienced from tests [5].

In the case of light weight concrete slabs the coefficient A in Eq. (14) equals to 1.32 just to account for the reduced value of the initial modulus of elasticity in stress block, and in addition, a reduction factor equal to 0.80 is adopted, to calculate the ultimate punching shear strength given by Eq. (7).

6.2. Steel

The modulus of elasticity of steel E is taken equal to 200 GPa whereas the value of yield stress used is the nominal one, for the sake of comparable predictions. In addition the value of E_2 in Fig. 4, which expresses the strain hardening effect is taken equal to 5 GPa. The yield strain of steel and the modulus E_1 are given by

$$\varepsilon_y = 0.002 + f_y/E, \tag{17}$$

$$E_1 = \frac{0.20 f_y}{0.002 + 0.20 f_y/E}. \tag{18}$$

7. Effect of various parameters on punching shear

7.1. Compression reinforcement

It is well recognized that compression reinforcement has a negligible effect on ultimate strength especially in slab–column connections with large tension steel ratio, ρ. However, for realistic values of steel ratio, an increase in the compression reinforcement increases the ultimate capacity of the slabs.

In this analysis, the contribution of the compression steel is taken into account through the computation of the NA depth of the flexural section, X_f. This implies

Table 1
Observed ultimate loads compared with predictions

No.	Type	d (mm)	D (mm)	ρ (%)	f_y (MPa)	f_{cu} (MPa)	X_f (mm)	X (mm)	V_{test} (kN)	Mode of failure	V_{calc} (kN)	V_{calc}/V_{test}
1	N.W.	98.	150.	0.58	550.	110.3	6.71	10.53	224.0	F	201.1	0.898
2	N.W.	98.	150.	0.58	550.	70.2	9.89	14.10	212.0	FP	199.2	0.940
3	N.W.	98.	150.	0.58	550.	33.6	17.67	20.53	169.0	P	177.5	1.051
4	N.W.	98.	150.	0.58	550.	73.4	9.51	13.71	233.0	F	199.6	0.856
5	L.W.	98.	150.	0.58	550.	68.0	11.50	15.65	190.0	P	173.3	0.912
6	N.W.	98.	150.	0.58	550.	127.3	5.95	9.58	233.0	F	201.3	0.864
12	N.W.	98.	150.	1.28	550.	75.5	18.65	21.18	319.0	P	314.2	0.985
13	N.W.	98.	150.	1.28	550.	54.3	24.10	24.30	297.0	P	289.4	0.974
14	N.W.	98.	150.	1.28	550.	76.0	18.55	21.12	341.0	P	314.7	0.923
15	L.W.	98.	150.	1.28	550.	85.5	19.28	21.58	276.0	P	278.2	1.008
16	N.W.	98.	150.	1.28	550.	123.0	13.10	17.07	362.0	P	350.7	0.969
21	N.W.	98.	150.	1.28	650.	52.4	28.59	26.39	286.0	P	306.9	1.073
22	N.W.	98.	150.	1.28	650.	105.3	16.55	19.76	405.0	P	365.9	0.903
23	N.W.	100.	150.	0.87	650.	70.5	16.31	19.74	341.0	P	283.6	0.832
24	L.W.	98.	150.	1.28	650.	55.8	30.05	26.99	270.0	P	261.9	0.970
25	N.W.	100.	150.	1.27	650.	41.1	35.50	29.34	244.0	P	294.1	1.205
26	N.W.	100.	150.	1.27	650.	47.0	31.70	27.96	294.0	P	306.5	1.042
27	N.W.	102.	150.	1.03	650.	42.1	29.24	27.24	227.0	P	281.2	1.239
Average of ratios (excluding slabs failing in flexure)												1.002
S.D.												0.109

Slabs tested by Ramdane [14].

Table 2
Observed ultimate loads compared with predictions

No.	Type	d (mm)	D (mm)	ρ/ρ' (%)	f_y (MPa)	f_{cu} (MPa)	X_f (mm)	X (mm)	V_{test} (kN)	Mode of failure	V_{calc} (kN)	V_{calc}/V_{test}
HS1	N.W.	95.	150.	0.49/0.42	490.	83.8	10.62	14.68	178.0	F	228.6	1.284
HS2	N.W.	95.	150.	0.84/0.42	490.	87.5	13.66	17.35	249.0	P	278.2	1.117
HS3	N.W.	95.	150.	1.47/0.42	490.	86.3	18.68	20.91	356.0	P	332.2	0.933
HS4	N.W.	90.	150.	2.37/0.44	490.	82.5	25.06	23.71	418.0	P	353.0	0.844
HS5	N.W.	125.	150.	0.64/0.32	490.	85.0	14.24	19.57	365.0	P	371.4	1.018
HS6	N.W.	120.	150.	0.94/0.33	490.	87.5	16.97	21.68	489.0	P	407.7	0.834
HS7	N.W.	95.	150.	1.19/0.42	490.	92.5	16.15	19.23	356.0	P	320.0	0.899
HS8	N.W.	120.	150.	1.11/0.33	490.	86.3	18.63	22.99	436.0	P	428.1	0.982
HS9	N.W.	120.	150.	1.61/0.33	490.	92.5	22.46	25.69	543.0	P	501.2	0.923
HS10	N.W.	120.	150.	2.33/0.33	490.	100.0	27.95	28.94	645.0	P	594.8	0.922
HS11	N.W.	70.	150.	0.95/0.57	490.	87.5	11.64	13.98	196.0	F	185.5	0.947
HS12	N.W.	70.	150.	1.52/0.57	490.	93.8	14.11	15.63	258.0	P	217.1	0.842
HS13	N.W.	70.	150.	2.00/0.57	490.	85.0	17.27	17.38	267.0	P	226.3	0.848
HS14	N.W.	95.	220.	1.47/0.42	490.	90.0	18.26	20.64	498.0	P	391.6	0.786
HS15	N.W.	95.	300.	1.47/0.42	490.	88.8	18.39	20.73	560.0	P	451.4	0.806
NS1	N.W.	95.	150.	1.47/0.42	490.	52.5	24.77	24.25	320.0	P	276.6	0.864
NS2	N.W.	120.	150.	0.94/0.33	490.	37.5	26.79	28.30	396.0	P	302.5	0.764
Average of ratios (excluding slabs failing in flexure)												0.892
S.D.												0.094

Slabs tested by Marzouk and Hussein [15].

Table 3
Observed ultimate loads compared with predictions

No.	Type	d (mm)	D (mm)	ρ/ρ' (%)	f_y (MPa)	f_{cu} (MPa)	X_f (mm)	X (mm)	V_{test}(kN)	Mode of failure	V_{calc} (kN)	V_{calc}/V_{test}
ND65-1-1	N.W.	275.	200.	1.49/0.00	500.	80.0	53.08	59.91	2050	P	2132.6	1.040
ND65-2-1	N.W.	200.	150.	1.75/0.00	500.	87.5	41.48	45.34	1200	P	1253.8	1.045
ND95-1-1	N.W.	275.	200.	1.49/0.00	500.	105.0	43.56	53.33	2250	P	2275.6	1.011
ND95-1-3	N.W.	275.	200.	2.55/0.00	500.	112.5	65.74	67.21	2400	P	3003.2	1.251
ND95-2-1	N.W.	200.	150.	1.75/0.00	500.	110.0	35.10	41.24	1100	P	1328.4	1.208
ND95-2-1D	N.W.	200.	150.	1.75/1.75	500.	108.8	37.70	42.99	1300	P	1374.1	1.057
ND95-2-3	N.W.	200.	150.	2.62/0.00	500.	112.5	48.96	49.48	1450	P	1617.6	1.116
ND95-2-3D	N.W.	200.	150.	2.62/1.75	500.	100.0	47.14	48.53	1250	P	1466.8	1.173
ND95-2-3D+	N.W.	200.	150.	2.62/1.75	500.	122.5	43.33	46.43	1450	P	1606.5	1.108
ND95-3-1	N.W.	88.	100.	1.84/0.00	500.	106.3	16.52	18.87	330	P	288.3	0.874
ND115-1-1	N.W.	275.	200.	1.49/0.00	500.	140.0	35.76	47.05	2450	P	2432.4	0.993
ND115-2-1	N.W.	200.	150.	1.75/0.00	500.	148.8	28.51	36.32	1400	P	1430.3	1.022
ND115-2-3	N.W.	200.	150.	2.62/0.00	500.	135.0	42.91	46.19	1550	P	1705.2	1.100
LWA75-1-1	L.W.	275.	200.	1.49/0.00	500.	86.3	56.97	62.31	1600	P	1865.7	1.166
LWA75-2-1	L.W.	200.	150.	1.75/0.00	500.	87.5	47.22	48.57	950	P	1074.4	1.131
LWA75-2-1D	L.W.	200.	150.	1.75/1.75	500.	92.5	42.49	45.94	1100	P	1054.6	0.959
LWA75-2-3	L.W.	200.	150.	2.62/0.00	500.	92.5	65.20	56.60	1150	P	1299.2	1.130
LWA75-2-3D	L.W.	200.	150.	2.62/1.75	500.	92.5	52.61	51.27	1020	P	1176.9	1.154
LWA75-3-1	L.W.	88.	100.	1.84/0.00	500.	85.0	22.14	22.07	320	P	232.4	0.726
Average of ratios												1.066
S.D.												0.123

Slabs tested by Tomaszewicz [16].

Table 4
Observed ultimate loads compared with predictions

No.	Type	d (mm)	D (mm)	ρ (%)	f_y (MPa)	f_{cu} (MPa)	X_f (mm)	X (mm)	V_{test} (kN)	Mode of failure	V_{calc} (kN)	V_{calc}/V_{test}
S2.1	N.W.	200.	250.	0.80	600.	30.2	56.07	52.86	603.0	P	816.0	1.353
S2.2	N.W.	199.	250.	0.80	600.	28.6	58.46	53.75	600.0	P	797.0	1.328
S2.3	N.W.	200.	250.	0.34	600.	31.7	25.53	33.80	489.0	P	538.9	1.102
S2.4	N.W.	197.	250.	0.35	600.	30.2	26.75	34.67	444.0	P	529.5	1.193
Average of ratios												1.244
S.D.												0.118

Slabs tested by Tolf [17].

Table 5
Observed ultimate loads compared with predictions

No.	Type	d (mm)	D (mm)	ρ (%)	f_y (MPa)	f_{cu} (MPa)	X_f (mm)	X (mm)	V_{test} (kN)	Mode of failure	V_{calc} (kN)	V_{calc}/V_{test}
HSC0	N.W.	200.	250.	0.80	600.	112.9	20.20	28.77	965.0	P	1068.6	1.107
HSC1	N.W.	200.	250.	0.80	600.	106.8	21.17	29.74	1021.0	P	1064.2	1.042
HSC2	N.W.	194.	250.	0.82	600.	98.8	22.19	30.44	889.0	P	1012.3	1.139
HSC4	N.W.	200.	250.	1.19	600.	98.8	31.27	38.48	1041.0	P	1307.1	1.256
HSC6	N.W.	201.	250.	0.60	600.	105.7	16.08	24.37	960.0	P	869.4	0.906
NHSC8	N.W.	198.	250.	0.80	600.	100.0	21.99	30.46	944.0	P	1035.9	1.097
HSC9	N.W.	202.	250.	0.33	600.	86.8	10.53	17.42	565.0	P	546.7	0.968
Average of ratios												1.073
S.D.												0.115

Slabs tested by Hallgren [5].

that in slabs with low tension steel ratios, the compression reinforcement, in reality, "works" in tension, and therefore an increase in its amount prevents the upward movement of the NA depth, X_f, resulting in increased punching shear strength.

7.2. Different tension steel ratios in orthogonal directions

The case of a slab with different tension steel ratios in x and y directions, ρ_x and ρ_y, respectively, can be accommodated by computing two different values of the flexural critical section depth X_{fx} and X_{fy} , corresponding to ρ_x and ρ_y, respectively. Thus, Eq. (9) takes the form

$$\frac{1}{X} = \frac{1}{2X_s} + \frac{1}{X_{fx} + X_{fy}}. \tag{19}$$

7.3. Concentration of tension reinforcement

The concentration of tension reinforcement under the column can be accounted for through the computation of X_f, based on new tension steel ratio.

8. Outline of analysis procedure

1. Determine the NA depth of the flexural section, X_f, taking into account the strain hardening effect, Eq. (13)

   $$X_f = \frac{\rho f_s - \rho' f'_s}{k_1 f_{cu}} d.$$

2. Determine the NA depth of the shear section, X_s, Eq. (10)

   $$X_s = 0.25d.$$

3. Determine the "mean" NA depth of the compression zone, Eq. (9)

   $$X = \frac{2X_s X_f}{X_s + X_f}.$$

4. Determine the splitting tensile strength of concrete, Eq. (15)

   $$f_{ct} = 0.27 f_{cu}^{2/3}.$$

5. Determine the critical perimeter, Eqs. (6.1) and (6.2)

   $b_p = 4r + 12d$ for square column

   $b_p = 4D + 12d$ for circular column

6. Calculate the ultimate punching shear strength of the slab, Eq. (7)

   $V_{calc} = b_p X \cot 30° f_{ct}$ for normal density concrete,

   $V_{calc} = 0.80 b_p X \cot 30° f_{ct}$ for light weight concrete.

9. Verification of the proposed model

The proposed model was applied to predict the ultimate strength of normal weight concrete test slabs reported in the literature (i.e., tests other than those of the authors) and failing in punching shear, where either the steel reinforcement ratio or the concrete strength was systematically varied. The results, not shown here, indicate that there exists a very good correlation between theoretical and observed strengths [13]. In this paper, the model has been applied to 60 tests, again other than those of the authors, to predict the punching strength of high concrete strength slabs mainly. The geometry of test slabs, analysis and the results are shown in Tables 1–5 and include 15 test results of Ramdane [14] with concrete strength varying from 40 to 127 MPa, 15 test results of Marzouk and Hussein [15] with concrete strength varying from 85 to 100 MPa mainly, 19 test results of Tomaszewicz [16] with concrete strength varying from 80 to 148 MPa, four test results of Tolf [17] with normal strength and seven test results of Hallgren [5] with concrete strength varying from 87 to 113 MPa. Tests made by Ramdane [14] and Tomaszewicz [16] include both normal density and lightweight concrete slabs.

For the proposed model, the overall average theory/test ratio was 1.020 with a S.D. of 0.142, giving strong support to the ability of the theory to explain the structural differences in slabs. It is therefore concluded that the model appears to be equally valid for high strength concrete slabs as for normal strength slabs.

It is also worth emphasizing that the slabs analyzed and presented in Tables 1–5 cover many variables that influence shear behavior such as the type of concrete, concrete strength, tension steel ratio and the size of loaded area. Bearing this in mind as well as the fact that the tests themselves are one-to-one scale models of the prototype, and the inevitable scatter of test results in concrete behavior, the theoretical model developed here is an excellent representation of the physical behavior of slab connections. It should also be noted that all the tests used to validate the theory were carried out quite independently over several years prior to the development of the theoretical concepts.

9.1. Comparison between present model and Hallgren's theory

In this section, an effort is made to compare the predicted strengths of the present model with those predicted by Hallgren's theory [5]. For the sake of comparison, the predicted strengths of the present model are calculated on the basis of the same mechanical

Table 6
Observed ultimate loads compared with predictions according to (a) present theory[a] (b) Hallgren's theory

Author	Total number of slabs	$V_{calc.}/V_{test}$	
		Average of ratios/S.D.	
		Present theory[a]	Hallgren's theory
Ramdane [14]	15	0.921/0.122	0.901/0.118
Marzouk and Hussein [15]	15	0.826/0.078	0.869/0.087
Tomaszewicz [16]	19	0.982/0.119	0.985/0.085
Tolf [17]	4	1.140/0.137	1.056/0.030
Hallgren [5]	7	0.915/0.113	0.941/0.104
	60	0.930/0.135	0.938/0.106

Steel strain hardening is not taken into account.
[a] $f_{ct} = 0.26 f_{cu}^{2/3}$ instead of $0.27 f_{cu}^{2/3}$.

properties of materials used in [5]. Thus, the strain hardening effect is not taken into account (i.e., $E_2 = 0$) and for the tensile strength of concrete the following relationship is used:

$$f_{ct} = 0.26 f_{cu}^{2/3}.$$

The predicted strengths of the slab–column connections according to the analysis of both models, based on the above common assumptions, are shown in Table 6. It is readily seen that the predictions of both models are on the safe side and quite comparable.

10. Conclusions

A simple engineering model is presented to predict the ultimate strength of reinforced concrete slab–column connections failing in punching shear. The model incorporates a good representation of the physical behavior, under load, of the connections made from lightweight concrete, and normal weight of both normal and high strength concrete. Punching is considered as a form of shearing and splitting without concrete crushing; failure is thus assumed to occur in the comparison zone above the inclined cracking when the limiting shear stress equals the tensile splitting strength of concrete. The method thus involves the computation of the depth of the compression zone and incorporates the inclination of the fracture surface, which reflect the influence of many of the parameters which affect the punching strength. Dowel action is taken into account by a using a critical parameter larger than the column perimeter.

The calculated punching shear strengths are compared with a large number of test results from various investigations, and show very good agreement with experimental results. The slabs analyzed cover many variables that influence shear behavior and mainly slabs made with high strength concrete.

References

[1] Regan PE, Braestrup MW. Punching shear in reinforced concrete. A State of the Art Report. Comite Euro-International, Lausanne, CEB-Bulletin No 168; 1985.
[2] Alexander SDB, Simmonds SH. Ultimate strength of slab–column connections. ACI Struct J 1987:255–61.
[3] Bazant ZP, Cao Z. Size effect in punching shear failure of slabs. ACI Struct J 1987;84(1):44–51.
[4] Gonzalez-Vidosa F, Kotsovos MD, Pavlovic D. Symmetrical punching of reinforced concrete slabs: an analytical investigation based on nonlinear Finite Element modeling. ACI Struct J 1998;85(3):241–50.
[5] Hallgren M. Punching shear capacity of reinforced high strength concrete slabs, Bulletin No 23. Department of Structural Engineering, KTH, Stockholm; 1996.
[6] Swamy RN, Andriopoulos AD. Contribution of aggregate interlock and dowel forces to the shear resistance of R.C. beams with web reinforcement. ACI Publ 1974;SP-42:129–66.
[7] Bauman T, Rüsch H. Versuche zum Studium der Verdübelungswirkung der Biegezugbewehrung eines Stahlbetonbalkens. In: Deutcher Ausschuß für Stahlbeton, Heft 210. Berlin: Ernst & Sohn; 1970. p. 43–83 (in German).
[8] Humadi YD, Regan PE. Behaviour in shear of beams with flexural cracks. Mag Concr Res 1980;32:67–78.
[9] BS 8110. The structural use of concrete. British Standard Institution; 1985.
[10] Regan PE. A comparison of British and ACI 318-71 treatments of punching shear. ACI Publ 1974;SP-42:881–904.
[11] The shear strength of reinforced concrete members-Slabs ASCE-ACI Committee 426. Structural J 1974. p. 1543–90.
[12] Mphonde AG, Frantz GC. Shear tests of high- and low-strength beams without stirrups. ACI Struct J 1984;81(4):350–7.
[13] Theodorakopoulos DD, Swamy RN. An engineering model to predict the punching shear strength of RC slabs. In: Proceedings of the International Workshop on Punching Shear, Stockholm. 2000. p. 91–8.
[14] Ramdane K-E. Punching shear of high performance concrete slabs. In: Proceedings of the 4th International Symposium on Utilization of High Strength High Performance Concrete, Paris. 1996. p. 1015–26.
[15] Marzouk H, Hussein A. Experimental investigation on the behaviour of high-strength concrete slabs. ACI Struct J 1991; 88(6):701–13.

[16] Tomaszewicz A. High-strength concrete. SP2-plates and shells. Report 2.3. Punghing Shear Capacity of Reinforced Concrete Slabs. Report No. STF70 A93082, SINTEF Structures and Concrete, Trondheim; 1993. 36 p.

[17] Tolf P. Plattjocklekens inverkan påbetongplattors hå llfasthet vid genomstansning. Försök med cikulära plattor. Bulletin 146. Department of Structural Mechanics and Engineering, KTH, Stockholm; 1998. 64 p. (in Swedish with summary in English).